Published in final edited form as:
Virology. 2012 April 10; 425(2): 122–132. doi:10.1016/j.virol.2012.01.005.

An intermediate dose of LCMV clone 13 causes prolonged morbidity that is maintained by CD4+ T cells

Andrew Stamm[1,3], **Laura Valentine**[1,3], **Rashaun Potts**[2], and **Mary Premenko-Lanier**[1]

[1]University of California San Francisco, Division of Experimental Medicine, 1001 Potrero Avenue, San Francisco, CA 94110

[2]San Francisco State University, Department of Biology, 1600 Holloway Avenue, San Francisco, CA 94132

Abstract

Wasting is a sign of various underlying disorders and is a common feature of cancer, sepsis, and AIDS. We have developed an in vivo model to study the various stages of wasting following infection of mice with lymphocytic choriomeningitis virus cl-13. Using this model we have identified four distinct stages of wasting and have discovered that all stages occur in the different groups of mice regardless of whether the virus is cleared or persists. However, the degree and extent of wasting varies between groups of mice, depending upon the dose of virus administered. Blocking IFNγ or TNFα, which are believed to take part in the wasting process, did not affect the wasting state. Finally, we found that CD4+ T cells control the maintenance stage of wasting. We believe this model will be useful in studying the regulation of wasting during a persistent viral infection, hopefully leading to improved therapies to ameliorate the disorder.

Keywords

Virus dose; LCMV; cl-13; persistent infection; CD4+ T cells; wasting; cachexia; TNFα; IFNγ

INTRODUCTION

Individuals infected with viruses experience a loss in their quality of life. This loss may be short and transient, such as following an influenza virus infection, or may be life-long, as occurs with a persistent HIV or hepatitis infection. The host response to a virus infection is generally responsible for morbidity and mortality. Host responses to an infection that impact the quality of life include fever, malaise, and weight loss. Therefore, understanding how the host response to infection is controlled may provide needed targets to biologically reverse the wasting process, increase the quality of life, and decrease deaths related to wasting in persons infected with acute or chronic viral infections world-wide.

Wasting is a syndrome associated with many diseases (Delano and Moldawer, 2006; Doehner and Anker, 2002; Inagaki, Rodriguez, and Bodey, 1974; Tisdale, 2002) such as

Corresponding author: Mary Premenko-Lanier, Phone: 415-206-8321, fax 415-206-8199, premenko-lanierm@medsfgh.ucsf.edu.
[3]These authors contributed equally to the project

cancer, congestive heart failure, chronic obstructive pulmonary disease, HIV, and tuberculosis (TB). The components of wasting include weight loss, anorexia, depletion of both fat and protein masses, muscle atrophy, gain in the proportion of body water, and a variety of metabolic changes (Langstein and Norton, 1991; Norton, Peacock, and Morrison, 1987). Indirect evidence for the role of cytokines has been derived from studies in which chronic administration of cytokines mimics wasting (Fong et al., 1989; Tracey et al., 1988). More specifically, evidence that TNFα has a role in wasting come from experiments in which the wasting syndrome associated with infections or with tumors is attenuated by treatment with antibodies to neutralize TNFα (Costelli et al., 1993; Gelin et al., 1991; Langstein et al., 1991; Sherry et al., 1989; Truyens et al., 1995; Yoneda et al., 1991). However, in many of these studies the administration of anti-TNFα antibodies not only reduces wasting, but also either reduced tumor size or parasitsemia. Therefore, it is difficult to determine what the biological effect of anti-TNFα treatment is in these studies.

Additional cytokines have been implicated in wasting. IL-1 has been shown to induce wasting in rats, similar to TNFα and LPS (Fong et al., 1989). While IL-6 has been shown to suppress the development of wasting associated with tumor growth (Strassmann et al., 1992). TNFα, IL-1, and IL-6 are triggers of the acute phase response that is implicated in many diseases (Hirano, 1994). It is the prevailing hypothesis that wasting develops as a result of chronic overstimulation induced by several cytokines acting in concert and affecting many different cells and organ systems. However, antagonism of one or all of these cytokines has not proven clinically beneficial in reversing the wasting state (Delano and Moldawer, 2006). Therefore, investigations into the mechanisms responsible for the development of wasting are needed.

LCMV cl-13 is an established model of a persistent virus infection (reviews; (Asano and Ahmed, 1995; Oldstone, 2002; Oldstone, 2006; Oldstone et al., 1985; Yi, Cox, and Zajac)). The LCMV model has led to the development of experimental therapies to treat persistent infections (Finnefrock et al., 2009; Larrubia et al., 2009) and towards understanding of the differences between acute and persistent viral infections (Wherry et al., 2003). LCMV has been used to study virus induced wasting (Doherty, Hou, and Southern, 1993; Kamperschroer and Quinn, 2002; Zajac et al., 1996; Zhou et al., 2009). From these LCMV wasting studies it was found that TNFα does not play role (Kamperschroer and Quinn, 2002) in the virus induced wasting, and that CD4+ T cells were important in the wasting process when CD8+ T cells were not present or the virus was injected intracranial (Doherty, Hou, and Southern, 1993; Fung-Leung et al., 1991; Zajac et al., 1996; Zhou et al., 2009). Though CD4+ T cells have been shown to be important in LCMV induced wasting, their role in the process is poorly understood.

Much of our knowledge about the mechanism of wasting is indirect, detecting serum levels of cytokines or forcing cachexia by continuous administration of a variety of cytokines or stimulants such as LPS. Therefore, in vivo models of wasting in natural infections are needed. We have used the LCMV model as a tool to study the infection-induced wasting state in vivo. This model has the potential to be valuable in dissecting the mechanism of this clinically important, debilitating process. We have found that wasting occurs in four distinct phases: 1) initiation, 2) decline, 3) recovery, and 4) maintenance. Our data suggest that each stage is independently regulated and that specific therapies to target each stage may be possible. Specifically, our data expand on the role that CD4+ T cells play during the wasting syndrome.

RESULTS

An intermediate dose of cl-13 leads to enhanced morbidity

We investigated the effect of 5-fold differences in the infectious dose on morbidity after cl-13 infection. We made five-fold dilutions of cl-13, using a very high (1×10^7 pfu), high (2×10^6 pfu), intermediate (4×10^5 pfu), and low (8×10^4 pfu) dose of virus to infect C57BL/6 mice intravenously. Mice infected with different doses of cl-13 had strikingly different patterns of morbidity (Figure 1a). All animals lost a small amount of body weight during the first two days of infection, and then recovered. They then underwent a second round of body weight loss beginning 6 days post infection. Differences in morbidity between the groups were observed by 8 days post-infection. In this second wave of weight loss, mice infected with a low dose of cl-13 lost significantly less body weight than all other groups of mice, and regained this body weight by day 10 post infection (Figure 1a, $p=0.001$ two-way ANOVA). Mice infected with high (2×10^6) or very high (1×10^7) doses of virus experienced wasting typical of cl-13 infected mice, losing about 20% of their body weight by day 8 post-infection. To our surprise, mice infected with the intermediate dose of cl-13 experienced enhanced wasting and prolonged morbidity relative to the higher and lower virally infected groups (Figure 1a, open circles).

Differences in the clinical outcome were also apparent in illness scores. Animals infected with the intermediate dose of virus showed high illness scores until about 16 days post-infection as compared to animals given the higher doses (Figure 1b). Intriguingly, animals given the low dose of cl-13 did not experience apparent illness beyond their moderate weight loss (Figure 1b), though the initial infectious dose was only five-fold lower than the dose causing the greatest illness. Mice infected with the rapidly cleared LCMV Armstrong strain at 2×10^6 pfu i.v., had a similar disease course as compared to the low dose LCMV cl-13 infection (data not shown).

Having observed this dose-dependent pattern of morbidity and illness in LCMV cl-13 infected mice we investigated whether variation in disease was due simply to corresponding changes in viral load. Mice were bled weekly and titers in the plasma were determined by plaque assay. At one week post-infection almost all mice infected with the low dose of virus had undetectable plasma viremia (Figure 1c), similar to what is seen using the less pathogenic Armstrong strain of LCMV, (Wherry et al., 2003) and from our own experiments with Armstrong (data not shown). Mice infected with intermediate, high and very high doses of virus had similar titers of LCMV in their plasma at weeks 1, 2 and 3 post-infection (Figure 1c). Mice infected with low dose cl-13 were able to control virus in all infected tissues between 15–22 days post infection (data not shown) whereas mice infected will all other doses of the same virus inoculum had virus titers measurable in the kidney (Figure 1d) and brain (data not shown) out to day 60 post infection. Thus, differences in viral titers by the first week of infection did not explain the differences in wasting observed in the medium, normal, and high dose groups at this time.

Viral titers are controlled very early in low dose-infected mice but do not fully explain differences in morbidity

We reasoned that events occurring early following infection may determine the morbidity differences that emerged at day 8 post-infection. Therefore, we closely examined the relationship between virus dose and very early kinetics of tissue viral loads. By day 5 post infection, there were no significant differences in viral titers measured between all groups of cl-13 infected mice (data not shown). By day 6 in the liver, the low dose infected mice had significantly lower levels of virus that continued through day 8 of the infection (Figure 2). This pattern was also true in the brain but not the kidney (Figure 2). On day 8 post infection,

the low dose group viral titers in the kidney were not significantly different then the other infected groups of mice. Mice infected with the intermediate and high doses of virus had increasing levels of virus in the brain on days 7 and 8 post infection, while low dose mice rapidly established control of viral replication in the brain.

Overall, mice infected with the low dose of cl-13 had significantly reduced viral titers in all tissues tested, indicating that a systemic infection was transiently established and then rapidly cleared. Also of interest, the intermediate dose groups' viral titers in tissues were similar to or lower than the high dose group at these early time points. By day 15, cl-13 was cleared from the low dose infected mice and there was no significant difference between the intermediate and high dose infected animals (data not shown). Thus, the prolonged morbidity and illness observed in the intermediate dose group as compared to the high dose group cannot be explained by greater amounts of virus replicating in their tissues.

Differences type I IFN production and CD69 expression on CD4+ and CD8+ T cells

We next hypothesized that immunological events within the first week of infection determined the course of disease. Since clearance of LCMV requires CD8+ T cells (Moskophidis et al., 1987), we examined T cell responses over time in the blood. All groups experienced a similar drop in total CD8+ T cells in the blood during the first 3 days after infection (data not shown). Other groups have attributed this early attrition of T cells to type I interferon (IFN-I) (Bahl et al., 2006). Mice infected with the low dose cl-13 had a significantly lower IFN-I response in the plasma compared to those infected with higher doses of cl-13 (Figure 3a, one way ANOVA p= 0.006). Type I IFN levels waned over time and are undetectable in all groups on days 5–8 post-infection (data not shown). The significantly reduced levels of type I IFN in the low dose infected group of mice correlated with their reduced levels of CD69 expression on both CD4+ and CD8+ T cells (Figure 3b–d). CD69 is upregulated non-specifically on T cells following an LCMV infection, probably in response to IFN-I (Shiow et al., 2006).

Mice infected with low dose cl-13 have more peripheral total CD8+ and CD4+ T cells and altered patterns of PD-1 expression

By day 8 post-infection, the low dose group had significantly elevated numbers of CD8+ cells (Figure 4a, p=0.0001 one way ANOVA), LCMV-specific GP33-tetramer positive cells (Figure 4b, p=0.0001, one-way ANOVA) and CD4+ T cells in the blood (Figure 4c, p= 0.0001, one-way ANOVA). CD8+ T cell counts in the other groups of LCMV-infected mice rebounded to normal levels by day 8, but were not significantly different from each other. Therefore, mice infected with 8×10^4 pfu of cl-13 had increases in both CD4+ T cells and CD8+ T cells while all other groups showed equivalent (or lower) CD4+ T cell and CD8+ T cell counts in the blood. This increase in absolute counts in low-dose infected mice appeared to be due to expansion of LCMV-specific cells.

Following activation, antigen specific T cells upregulated PD-1 (Barber et al., 2006). Interestingly, we noticed that mice infected with the low dose of cl-13 had differences in PD-1 expression on CD8+ and CD4+ T cells. PD-1 was expressed on the CD4+ T cell effector population ($CD44^{+}CD62L^{Lo}$) in mice infected with the low dose of virus at 1 and 2 weeks post infection and then significantly down regulated by 3 weeks post infection (Figure 4d and e, p=0.0001 one way ANOVA). On CD8+ T cells we observed a different pattern of PD-1 expression: by day 8 post-infection, CD8+ T cells from mice given the low dose of cl-13 had significantly lower levels of PD-1 expression than CD8+ T cells from mice infected with the higher doses of virus (Figure 4f and g, p=0.001 one way ANOVA). The difference in PD-1 MFI appeared to be due to lower levels of PD-1 expressed on LCMV-specific CD8+ T cells, as revealed by staining with a GP33-specific tetramer (Figure

4h and i, p=0.0001 one way ANOVA). Virus is still present in the organs of the low dose-infected mice at this time (Figure 2), so these data indicate that PD-1 down regulation on CD8+ T cells does not strictly correlate with clearance of the viral antigen (Sharpe et al., 2007).

With respect to the high and very high dose groups (2×10^6 and 1×10^7 pfu), PD-1 expression was not significantly altered between weeks 1–3 post infection. We did detect a significant difference in the level of PD-1 expression on CD4+ T cells that were $CD44^{high}$ $CD62L^{lo}$ (effector cells) in the intermediate (4×10^5 pfu) dose group 1-week post infection (Figure 4d and e). In addition, we found that mice infected with the intermediate dose of virus had a significant increase in the level of PD-1 expression on both CD8+ T effector cells and GP33-specific CD8+ T cells at week 2 post infection (Figure 4f and g, p=0.0004 and 0.0003 respectively, one way ANOVA). These data show that an increased frequency of activated, PD-1 expressing T cells was correlated with prolonged morbidity when present in conjunction with high levels of virus (Figure 1a).

An early CD4+ T cell response is followed by a significant expansion of the CD8+ T compartment in mice infected with the low dose of cl-13

Since differences between the peripheral T cell responses in the various groups of mice were evident by day 8 post-infection (Figure 4d–i), we decided to focus on early antigen-specific T cell responses. Mice were infected with low, intermediate, and high doses of cl-13 and sacrificed on days 6, 7, and 8 post-infection. These time points correspond divergence of different groups of mice in the extent of their weight loss. Functionality of antigen-specific splenic T cells was examined. At day 6 post-infection, both CD4+ and CD8+ T cell responses to immunodominant epitopes were readily detectable (Figure 5a, c–d). On day 6 post-infection, mice infected with the low dose made significantly larger CD4+ T cell responses to the GP61 epitope than those made by mice that received the intermediate and high doses of virus (Figure 5a and b, p=0.01 one-way ANOVA). The difference in magnitude of CD4+ T cell responses between low dose mice and the intermediate or high dose mice continued through day 8 post infection (Figure 5a). At that time the low dose-infected mice had GP61-specific responses, which were 3 to 5-fold larger in frequency than responses made by mice that received higher doses of virus. (Figure 5b, day 7 p=0.0043 and day 8 p=0.04, one-way ANOVA).

In the CD8+ T cell compartment, all groups of mice made responses against GP33 and NP396 of comparable frequency at day 6 post-infection, as measured by IFNγ/TNFα secretion in response to peptide (Figure 5c and d). However, the np396 response was significantly elevated in mice infected with low dose cl-13 as compared to mice infected with the very high dose. By days 7 and 8 post-infection though, the difference in the magnitude of the CD8+ T cell responses made by the low dose group and the other groups was dramatic (Figure 5e and f, Day 7 gp33 p=0.0001, np396 p=0.001 and day 8 gp33 p=0.03 and np396 p=0.01, one-way ANOVA). The low dose cl-13 infected mice made 2 to 10 fold higher frequency responses compared to intermediate and high dose groups. The magnitude of responses made by the intermediate and high dose groups were similar to each other.

In summary, mice infected with a low dose of cl-13 (8×10^4 pfu) had a higher frequency of CD4+ T cells 6 days post-infection as compared to mice infected with the intermediate or high doses. This divergence in CD4+ T cell response magnitude was followed by a divergence in the magnitude of CD8+ T cell responses on days 7 and 8 post infection (Figure 5b, e and f). These results indicate that the expansion phase of T cell responses against LCMV was affected by the initial dose of virus given, with a lower initial dose resulting in significantly larger T cell responses. This robust response occurred at the same

time viremia was being cleared in these animals and these mice experienced the least severe wasting (Figure 1a).

Measurement of pyrogens in plasma

The rapid clearance of virus observed in mice infected with the low dose of cl-13 was associated with reduced morbidity (Figure 1a). However, neither quantitation of early T cell responses nor of viral loads satisfactorily explained the enhanced morbidity experienced by the mice infected with an intermediate dose (4×10^5 pfu) as compared to mice that received higher doses of cl-13. This led us to quantitate the levels of plasma cytokines that have been previously implicated in immunopathology (Kamperschroer and Quinn, 2002) and referred to as pyrogens. Pyrogens are substances that induce a fever response. Well-characterized pyrogens include TNFα and IL-1β (Stefferl et al., 1996). We performed a Luminex assay to determine whether we could detect differences in cytokine levels known to be important in morbidity and wasting. From each dose group, we randomly tested six mice from two independent experiments for cytokine measurement and observed no differences in IL-6, IL-10, or IL-1β levels between the groups (data not shown). There was a peak of IFNγ production at day 6 post infection that was reduced at least five-fold by day 7 post infection in all groups of infected mice (Figure 6a). Interestingly, mice infected with 2×10^6 pfu had a significant reduction in circulating levels of IFNγ at day 6 as compared to the low dose infected mice (Figure 6a). We also detected increased levels of TNFα 6 days post infection in all infected groups (Figure 6b). In the low dose-infected group, this TNFα peak was reduced by day 7 and was undetectable by day 8. In contrast, TNFα levels were detectable in the plasma of mice infected with the normal or medium doses of cl-13 out to 15 days post infection (Figure 6b).

These data suggested that IFNγ and TNFα levels might have a role in the increased morbidity experienced by the mice infected with an intermediate dose of cl-13. We reasoned that blocking TNFα or IFNγ might thus ameliorate the prolonged morbidity. To test this hypothesis, mice were infected with 4×10^5 pfu of cl-13 and treated on days 5 and 7 with either IFNγ or TNFα neutralizing antibodies. Treatment had no effect on morbidity (Figure 6c) or viral titers (Figure 6d and 6e). Our results confirm previous studies using anti-TNFα antibodies during an LCMV infection (Kamperschroer and Quinn, 2002). Our lab has also used the IFNγ blocking antibody to successfully reverse the antiviral state following an in vivo cl-13 infection (unpublished data). Therefore, we believe that both blocking antibodies were used at a biologically relevant dose. Although levels of IFNγ and TNFα were elevated following infection with the different doses of cl-13, blocking these pyrogens individually was not sufficient to ameliorate morbidity. Therefore, IFNγ and TNFα have a role in inflammation, they do not individually influence wasting in our model.

CD4+ T cells maintain the wasting disease following the intermediate dose of cl-13

CD4+ T cells are known to play a role in morbidity following an LCMV infection (Doherty, Hou, and Southern, 1993; Fung-Leung et al., 1991; Zajac et al., 1996; Zhou et al., 2009). Therefore we wanted to investigate if CD4+ T cells were impacting wasting in our model. Since the wasting state initiates between days 5–6 in all groups, we tested whether depleting CD4+ T cells on day 5 following infection with the different doses of cl-13 would perturb morbidity. Depleting CD4+ T cells was effective following GK1.5 antibody administration five days post cl-13 infection (data not shown). Following depletion, CD4+ T cells reappear in the circulation within 1 week (data not shown). CD4+ T cell depletion did not affect the initiation of wasting state following cl-13 infection (Figure 7a–c). However, 5 days after depletion of CD4+ T cells the mice began to recover more rapidly than untreated infected controls (Figure 7a–c). By 11 days post infection mice depleted of CD4+ T cells have a significant increase in the body weight (Figure 7d). The recovery of body weight was

independent of virus loads because treated mice had the same levels of virus as untreated mice (Figure 7e and 7f). Clearance of the virus in the low dose infected group was not altered in CD4 depleted animals (data not shown). In addition CD8+ T cell responses were not altered when CD4+ T cells were depleted at this time (Figure 7g). These data suggest that the presence of CD4+ T cells is not required to initiate wasting, but CD4+ T cell are required to maintain the morbid state.

Discussion

Wasting is a debilitating, difficult to treat condition that is an essential part of the pathology of many diseases. Here we describe an in vivo model for dissecting the distinct stages of the wasting process (Figure 1). In our model, infection with different doses of the same virus leads to marked differences in the severity of morbidity. These differences were not explained completely by either differences in the levels of viremia or by the immune responses engendered, but appeared to be a result of the interaction of these two variables. We have found and confirmed that TNFα (Kamperschroer and Quinn, 2002) is not sufficient to drive wasting, despite its presence during cachexia.

The initial interactions of the pathogen and the host are critical. Our model demonstrates that the initial virus dose has an important role in determining the outcome of disease. We describe a system in which a potentially persistent viral infection is either cleared by the host without causing discernable illness, or establishes a persistent infection characterized by significant wasting and immune exhaustion. Diseases such as hepatitis C (HCV) (Lewis-Ximenez et al.), and hepatitis B (HBV) (Webster and Bertoletti, 2002) have similar diverse outcomes in humans. Once an infection has been established, it is difficult to determine whether immunological responses correlated with particular outcomes are causes or consequences of the persistent infection. Our model supports wasting as a common biological process regardless of whether the virus is cleared or persists.

Following administration of the lowest dose of cl-13, 8×10^4 pfu a systemic infection is established and then rapidly cleared by robust T cell responses with little apparent illness. However, administration of only five-fold more virus to mice results in sustained morbidity and the establishment of a persistent infection. Differences in virus load (Figure 1 and Figure 2) do not explain the differences in disease outcome between the intermediate and high dose infected groups. During the period of wasting, the virus load between the intermediate and high dose groups of mice is not significantly different although mice infected with the high dose of cl-13 recover more rapidly then mice infected with the intermediate dose of virus (Figure 1a).

It has been well established that T cells contribute to the pathology of LCMV infection. Therefore, we investigated whether differences in T cell responses could account for differences in wasting. PD-1 levels on CD4+ T cells 8 days following infection and PD-1 levels on CD8+ T cells 15 days post infection are significantly increased in mice infected with the intermediate dose of cl-13 as compared to all other groups of infected mice, (Figure 4d and 4f respectively) indicating greater T cell activation. Two weeks following infection, a time when PD-1 levels remain elevated in the intermediate dose group, the mice begin to recover from wasting. When CD4+ T cell PD-1 levels are significantly increased in the intermediate dose group 8 days post infection, mice are maintaining their morbid state. Therefore, altered CD4+ T cell activation 1 week post infection in the intermediate dose group may drive the enhanced wasting.

CD4+ T cells have also been implicated in wasting, but their exact role is unknown (Doherty, Hou, and Southern, 1993; Fung-Leung et al., 1991; Zajac et al., 1996; Zhou et al., 2009). Some of these published studies suggest that CD4+ T cells have a role in wasting

when CD8+ T cells are also depleted. These results demonstrate that without both CD4+ T cells and CD8+ T cells wasting does not occur. Using our model we found that depletion of CD4+ T cells led to a more rapid recovery from wasting in all mice infected with cl-13 regardless of dose, (Figure 7a–d) and independent of virus load (Figure 7e–f). Although, mice infected with the intermediate dose of cl-13 and depleted of their CD4+ T cells had the most significant difference in morbidity (Figure 7b), these mice do not normally recover from morbidity until 3 weeks following infection (Figure 1a). The low and high dose infected mice naturally have a period of recover (Figure 1a) and CD4+ T cell depletion accelerates this recovery period (Figure 7a and 7c). This suggests that CD4+ T cells contribute to the maintenance of wasting and further prevent mice infected with the intermediate dose of virus from entering a recovery period. It is important to point out that while there do not appear any obvious differences in the CD4+ T cell response following the intermediate and high doses of cl-13, the intermediate has a prolonged morbid state that CD4 depletion partially reverts. Therefore, other to be determined factors may also contribute in maintaining the morbid state. We are currently investigating whether the CD4+ T cell response transitions from an early effector to a regulatory response during the maintenance stage of wasting (Fahey et al.). Additionally, we have depleted CD8+ T cells in the low dose infected mice at 5 days following infection. CD8+ T cell depletion exasperated the morbid state (data not shown) and therefore was not attempted in the higher dose groups. Other cells such as antigen presenting cells may play a role in this complex process.

TNFα, also known as cachectin, is known to cause a lethal state of shock and a chronic wasting syndrome when produced in abundance (Araki et al., 2009; Beutler and Cerami, 1988). Pro-inflammatory cytokines play a role in LCMV wasting disease when the virus is administered by intracranial inoculation (Kamperschroer and Quinn, 2002). In the present study we found that both IFNγ and TNFα were elevated during the wasting state (Figure 6a–b). However, we did not find an obvious relationship between TNFα or IFNγ and the enhanced morbidity and wasting in mice infected with the intermediate cl-13 dose of 4×10^5 pfu (Figure 6c–e). Thus it is possible that the presence of these inflammatory cytokines during virus induced wasting may be correlative but not causative.

Using our model of LCMV cl-13 infection we propose that wasting occurs in 4 distinct stages: initiation, decline, recovery, and maintenance (Figure 8). Depending on the dose of the original inoculum, the time that each group enters a particular stage, or transitions to the next stage, is different. We did not find that increased viral titers necessarily corresponded to increased wasting. Nor did we find that mice that had a very strong T cell response experienced more wasting. Rather, the interaction of these two parameters may underlie the illness observed. Using this model, in which the same virus causes different degrees of pathology, we hope to further elucidate how the different stages of wasting are regulated in the context of a viral infection. This knowledge may then prove useful in developing interventions to ameliorate the symptoms associated with many diseases.

MATERIALS & METHODS

Mice and virus

Female wild type C57BL/6 mice were purchased from Charles River Laboratories (Wilmington, MA) and used at 6–8 weeks of age. All mice were maintained under specific pathogen-free conditions at the UCSF SFGH animal facility and were used in accordance with university animal welfare guidelines. LCMV cl-13 and Armstrong were a gift from Dr. Mehrdad Matloubian and were propagated on BHK cells. Age- and sex-matched animals were given 5-fold dilutions of cl-13 virus made in serum-free RPMI (8×10^4, 4×10^5, 2×10^6 or 1×10^7 pfu) by tail-vein injection. LCMV Armstrong was used at a dose of 8×10^4 or 2×10^6 pfu. Following infection, mice were weighed daily for the first month then weekly

thereafter. Body weight was calculated as a fraction of a mouse's starting body weight. Mice were scored for illness by giving a point for each of the following conditions: ruffled fur, weight loss exceeding 15%, visually lethargic, lethargic to the touch, and a hunched back. Mice were euthanized according to an approved IACUC protocol. Titers of virus were determined by plaque assay on Vero cells as previously described (Ahmed et al., 1984).

Type I IFN bioassay

Type I interferon bioassay was used to measure IFN-I as described (Cembrzynska-Nowak, 1989). The murine IFN standard (Biomedical Laboratories PBL, 12100-1) at a final concentration of 100U ml^{-1} was used as a control.

Sample collection, cell suspension and flow cytometry

Heparinized blood was collected by tail vein nick. The blood was spun down at 12000 rpm and the plasma collected for plaque and cytokine assays. Blood cells were then resuspended and stained for 15 minutes at room temperature with fluorochrome-conjugated antibodies. Fluorochrome-conjugated antibodies were obtained from BD Pharmingen (San Diego, CA), and eBiosciences (San Diego, CA). Red blood cells were lysed using BD FACS Lysing Solution (BD Biosciences, Franklin Lakes, NJ); cells were washed twice in FACS Buffer (PBS/1%BSA), and fixed (PBS/1% PFA) prior to running on a flow cytometer. Single cell suspensions of splenocytes were prepared by mashing the spleen through a 70 μm cell were lysed using ACK Buffer (Sigma-Aldrich, St Louis, MO) and washed with RPMI. For intracellular cytokine staining assays, splenocytes were resuspended in RPMI supplemented with 10% FCS (Hyclone) and stimulated with 2.5 μM peptide for 6 hours at 37 C in the presence of GolgiPlug (BD Biosciences). Cells were stained for surface and intracellular markers using the BD Cytofix/Cytoperm Kit following manufacturer's protocol. Tetramers (GP33) were by synthesized by the Microchemical Facility Core (Emory University, Atlanta, GA). Samples were read on an LSRII flow cytometer (BD Biosciences) and results were analyzed using FlowJo software (TreeStar, Ashland, OR).

Peptides

Peptides gp33-41 (KAVYNFATM), np366-374 (ASNENMDAM), gp61-80 (GLNGPDIYKGVYQFKSVEFD), were synthesized by Anaspec (Fremont, CA).

In vivo antibody treatment

CD4+ T cell depletion was done using the antibody clones GK1.5 at 500μg/mouse/dose administered at the indicated timepoints i.p. Anti-IFNγ antibodies were administered at 200 μg/mouse/dose at indicated time points i.p. Anti-TNFα antibodies were administered at 100 μg/mouse at the indicated time points. GK1.5, and anti-IFNγ antibodies were provided by the UCSF hybridoma core facility. Anti-TNFα antibodies was purchased from MyBioSource, (MBS670094, Rat Anti-Mouse TNF-a-LE/AF).

Luminex analysis

For Luminex assays, plasma was thawed at room temperature, gently vortexed, then centrifuged at 13,200 rpm for 10 min at 4°C immediately prior to testing. Cytokines were measured using a MILLIPLEX MAP High Sensitivity Mouse Cytokine Panel (7-plex, Millipore) according to the manufacturer's instructions. Plates were read on a Luminex-100 (Millipore) with Masterplex QT software (MiraiBio).

Statistical Analysis

Statistical significance was determined by Standard two tailed T-test or 1 or 2-way ANOVA, using Prism 5 (Graphpad Software, La Jolla, CA).

Acknowledgments

This work was funded in part by US National Institutes of Health R00 AI076346-01 and support was also provided by the Harvey V. Berneking Living Trust. We would like to thank JM. McCune (University of California, Department of Experimental Medicine), S. Kaech (Yale University) and P. Romangnoli (University of Connecticut) for very helpful discussions. We would like to thank Mehrdad Matloubian for providing the type I IFN receptor knockout mice. The DEM core laboratory generated the Luminex data. The DEM Core immunology Laboratory is supported by a grant from the National Center for Research Resources (NCRR) to the UCSF CTSI (UL1 RR024131).

References

Ahmed R, Salmi A, Butler LD, Chiller JM, Oldstone MB. Selection of genetic variants of lymphocytic choriomeningitis virus in spleens of persistently infected mice. Role in suppression of cytotoxic T lymphocyte response and viral persistence. J Exp Med. 1984; 160(2):521–40. [PubMed: 6332167]

Araki K, Turner AP, Shaffer VO, Gangappa S, Keller SA, Bachmann MF, Larsen CP, Ahmed R. mTOR regulates memory CD8 T-cell differentiation. Nature. 2009; 460(7251):108–12. [PubMed: 19543266]

Asano MS, Ahmed R. Immune conflicts in lymphocytic choriomeningitis virus. Springer Semin Immunopathol. 1995; 17(2–3):247–59. [PubMed: 8571171]

Bahl K, Kim SK, Calcagno C, Ghersi D, Puzone R, Celada F, Selin LK, Welsh RM. IFN-induced attrition of CD8 T cells in the presence or absence of cognate antigen during the early stages of viral infections. J Immunol. 2006; 176(7):4284–95. [PubMed: 16547266]

Barber DL, Wherry EJ, Masopust D, Zhu B, Allison JP, Sharpe AH, Freeman GJ, Ahmed R. Restoring function in exhausted CD8 T cells during chronic viral infection. Nature. 2006; 439(7077):682–7. [PubMed: 16382236]

Beutler B, Cerami A. Cachectin, cachexia, and shock. Annu Rev Med. 1988; 39:75–83. [PubMed: 3285792]

Cembrzynska-Nowak M. Different antiviral activity and cell specificity of interferon preparations produced by mouse peritoneal cells at 37 degrees C and at 26 degrees C. Arch Immunol Ther Exp (Warsz). 1989; 37(5–6):499–502. [PubMed: 2484831]

Costelli P, Carbo N, Tessitore L, Bagby GJ, Lopez-Soriano FJ, Argiles JM, Baccino FM. Tumor necrosis factor-alpha mediates changes in tissue protein turnover in a rat cancer cachexia model. J Clin Invest. 1993; 92(6):2783–9. [PubMed: 8254032]

Delano MJ, Moldawer LL. The origins of cachexia in acute and chronic inflammatory diseases. Nutr Clin Pract. 2006; 21(1):68–81. [PubMed: 16439772]

Doehner W, Anker SD. Cardiac cachexia in early literature: a review of research prior to Medline. Int J Cardiol. 2002; 85(1):7–14. [PubMed: 12163205]

Doherty PC, Hou S, Southern PJ. Lymphocytic choriomeningitis virus induces a chronic wasting disease in mice lacking class I major histocompatibility complex glycoproteins. J Neuroimmunol. 1993; 46(1–2):11–7. [PubMed: 8103060]

Fahey LM, Wilson EB, Elsaesser H, Fistonich CD, McGavern DB, Brooks DG. Viral persistence redirects CD4 T cell differentiation toward T follicular helper cells. J Exp Med. 208(5):987–99. [PubMed: 21536743]

Finnefrock AC, Tang A, Li F, Freed DC, Feng M, Cox KS, Sykes KJ, Guare JP, Miller MD, Olsen DB, Hazuda DJ, Shiver JW, Casimiro DR, Fu TM. PD-1 blockade in rhesus macaques: impact on chronic infection and prophylactic vaccination. J Immunol. 2009; 182(2):980–7. [PubMed: 19124741]

Fong Y, Moldawer LL, Marano M, Wei H, Barber A, Manogue K, Tracey KJ, Kuo G, Fischman DA, Cerami A, et al. Cachectin/TNF or IL-1 alpha induces cachexia with redistribution of body proteins. Am J Physiol. 1989; 256(3 Pt 2):R659–65. [PubMed: 2784290]

Fung-Leung WP, Kundig TM, Zinkernagel RM, Mak TW. Immune response against lymphocytic choriomeningitis virus infection in mice without CD8 expression. J Exp Med. 1991; 174(6):1425–9. [PubMed: 1683893]

Gelin J, Moldawer LL, Lonnroth C, Sherry B, Chizzonite R, Lundholm K. Role of endogenous tumor necrosis factor alpha and interleukin 1 for experimental tumor growth and the development of cancer cachexia. Cancer Res. 1991; 51(1):415–21. [PubMed: 1703040]

Hirano, T. The cytokine handbook. 2. Thomson, A., editor. Academic Press; 1994.

Inagaki J, Rodriguez V, Bodey GP. Proceedings: Causes of death in cancer patients. Cancer. 1974; 33(2):568–73. [PubMed: 4591273]

Kamperschroer C, Quinn DG. The role of proinflammatory cytokines in wasting disease during lymphocytic choriomeningitis virus infection. J Immunol. 2002; 169(1):340–9. [PubMed: 12077263]

Langstein HN, Doherty GM, Fraker DL, Buresh CM, Norton JA. The roles of gamma-interferon and tumor necrosis factor alpha in an experimental rat model of cancer cachexia. Cancer Res. 1991; 51(9):2302–6. [PubMed: 1901758]

Langstein HN, Norton JA. Mechanisms of cancer cachexia. Hematol Oncol Clin North Am. 1991; 5(1):103–23. [PubMed: 2026566]

Larrubia JR, Benito-Martinez S, Miquel J, Calvino M, Sanz-de-Villalobos E, Parra-Cid T. Costimulatory molecule programmed death-1 in the cytotoxic response during chronic hepatitis C. World J Gastroenterol. 2009; 15(41):5129–40. [PubMed: 19891011]

Lewis-Ximenez LL, Lauer GM, Schulze Zur Wiesch J, de Sousa PS, Ginuino CF, Paranhos-Baccala G, Ulmer H, Pfeiffer KP, Goebel G, Pereira JL, Mendes de Oliveira J, Yoshida CF, Lampe E, Velloso CE, Alves Pinto M, Coelho HS, Almeida AJ, Fernandes CA, Kim AY, Strasak AM. Prospective follow-up of patients with acute hepatitis C virus infection in Brazil. Clin Infect Dis. 50(9):1222–30. [PubMed: 20235831]

Moskophidis D, Cobbold SP, Waldmann H, Lehmann-Grube F. Mechanism of recovery from acute virus infection: treatment of lymphocytic choriomeningitis virus-infected mice with monoclonal antibodies reveals that Lyt-2+ T lymphocytes mediate clearance of virus and regulate the antiviral antibody response. J Virol. 1987; 61(6):1867–74. [PubMed: 3494855]

Norton JA, Peacock JL, Morrison SD. Cancer cachexia. Crit Rev Oncol Hematol. 1987; 7(4):289–327. [PubMed: 3123081]

Oldstone MB. Biology and pathogenesis of lymphocytic choriomeningitis virus infection. Curr Top Microbiol Immunol. 2002; 263:83–117. [PubMed: 11987822]

Oldstone MB. Viral persistence: parameters, mechanisms and future predictions. Virology. 2006; 344(1):111–8. [PubMed: 16364742]

Oldstone MB, Ahmed R, Byrne J, Buchmeier MJ, Riviere Y, Southern P. Virus and immune responses: lymphocytic choriomeningitis virus as a prototype model of viral pathogenesis. Br Med Bull. 1985; 41(1):70–4. [PubMed: 3882190]

Sharpe AH, Wherry EJ, Ahmed R, Freeman GJ. The function of programmed cell death 1 and its ligands in regulating autoimmunity and infection. Nat Immunol. 2007; 8(3):239–45. [PubMed: 17304234]

Sherry BA, Gelin J, Fong Y, Marano M, Wei H, Cerami A, Lowry SF, Lundholm KG, Moldawer LL. Anticachectin/tumor necrosis factor-alpha antibodies attenuate development of cachexia in tumor models. FASEB J. 1989; 3(8):1956–62. [PubMed: 2721856]

Shiow LR, Rosen DB, Brdickova N, Xu Y, An J, Lanier LL, Cyster JG, Matloubian M. CD69 acts downstream of interferon-alpha/beta to inhibit S1P1 and lymphocyte egress from lymphoid organs. Nature. 2006; 440(7083):540–4. [PubMed: 16525420]

Stefferl A, Hopkins SJ, Rothwell NJ, Luheshi GN. The role of TNF-alpha in fever: opposing actions of human and murine TNF-alpha and interactions with IL-beta in the rat. Br J Pharmacol. 1996; 118(8):1919–24. [PubMed: 8864524]

Strassmann G, Fong M, Kenney JS, Jacob CO. Evidence for the involvement of interleukin 6 in experimental cancer cachexia. J Clin Invest. 1992; 89(5):1681–4. [PubMed: 1569207]

Tisdale MJ. Cachexia in cancer patients. Nat Rev Cancer. 2002; 2(11):862–71. [PubMed: 12415256]

Tracey KJ, Wei H, Manogue KR, Fong Y, Hesse DG, Nguyen HT, Kuo GC, Beutler B, Cotran RS, Cerami A, et al. Cachectin/tumor necrosis factor induces cachexia, anemia, and inflammation. J Exp Med. 1988; 167(3):1211–27. [PubMed: 3351436]

Truyens C, Torrico F, Angelo-Barrios A, Lucas R, Heremans H, De Baetselier P, Carlier Y. The cachexia associated with Trypanosoma cruzi acute infection in mice is attenuated by anti-TNF-alpha, but not by anti-IL-6 or anti-IFN-gamma antibodies. Parasite Immunol. 1995; 17(11):561–8. [PubMed: 8817602]

Webster GJ, Bertoletti A. Control or persistence of hepatitis B virus: the critical role of initial host-virus interactions. Immunol Cell Biol. 2002; 80(1):101–5. [PubMed: 11869367]

Wherry EJ, Blattman JN, Murali-Krishna K, van der Most R, Ahmed R. Viral persistence alters CD8 T-cell immunodominance and tissue distribution and results in distinct stages of functional impairment. J Virol. 2003; 77(8):4911–27. [PubMed: 12663797]

Yi JS, Cox MA, Zajac AJ. T-cell exhaustion: characteristics, causes and conversion. Immunology. 129(4):474–81. [PubMed: 20201977]

Yoneda T, Alsina MA, Chavez JB, Bonewald L, Nishimura R, Mundy GR. Evidence that tumor necrosis factor plays a pathogenetic role in the paraneoplastic syndromes of cachexia, hypercalcemia, and leukocytosis in a human tumor in nude mice. J Clin Invest. 1991; 87(3):977–85. [PubMed: 1999505]

Zajac AJ, Quinn DG, Cohen PL, Frelinger JA. Fas-dependent CD4+ cytotoxic T-cell-mediated pathogenesis during virus infection. Proc Natl Acad Sci U S A. 1996; 93(25):14730–5. [PubMed: 8962123]

Zhou S, Kurt-Jones EA, Cerny AM, Chan M, Bronson RT, Finberg RW. MyD88 intrinsically regulates CD4 T-cell responses. J Virol. 2009; 83(4):1625–34. [PubMed: 19052080]

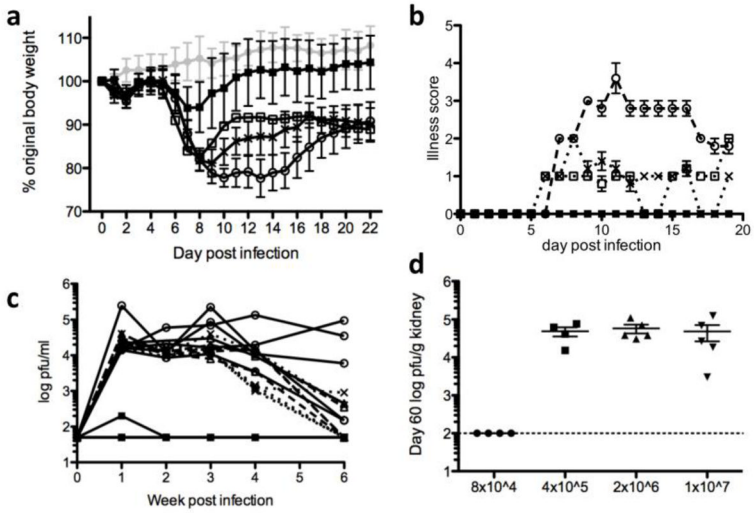

Figure 1. An intermediate dose of LCMV cl-13 leads to enhanced morbidity

Mice were infected with a low (8×10^4 pfu) (■), intermediate (4×10^5 pfu) (○), high (2×10^6 pfu) (X), or very high (1×10^7 pfu) (□) dose of LCMV cl-13 intravenously, or uninfected (grey line). **a**. Percent body weight loss following infection, pooled data from 5 independent experiments. Error bars = mean error + SD. p=0.0001 2-way ANOVA virus dose and % body weight loss were compared between 8–15 days post infection between the intermediate dose infection to all other groups of mice. **b**. Illness scores of mice infected with the different doses of cl-13. **c**. Plasma viral loads of individual animals infected with the different does of cl-13. **d.** Day 60 post-infection viral titers in the kidney. Dashed line indicates limit of detection. Results are representative of at least 3 independent experiments.

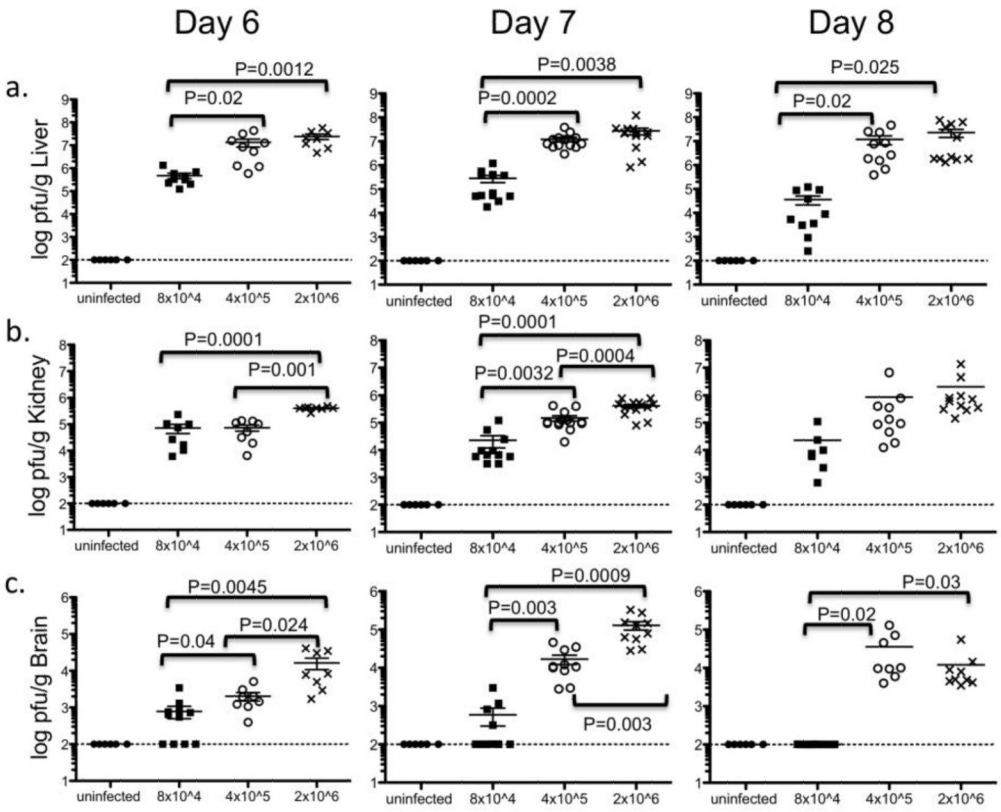

Figure 2. Virus replication is controlled early in the brain of mice infected with low dose cl-13

Mice were infected with a low (8×10^4 pfu, ■), intermediate (4×10^5 pfu, ○), or high (2×10^6 pfu, X) dose of LCMV cl-13 intravenously, or uninfected. LCMV titers in tissues were measured on Day 6 (first column), Day 7 (second column) and Day 8 (third column) post-infection in the liver (**a**), kidney (**b**) and brain (**c**) titers. All statistics were done using the student t-test. Data pooled from 2 independent experiment n=3–5 mice/group/experiment, error bars represent mean.

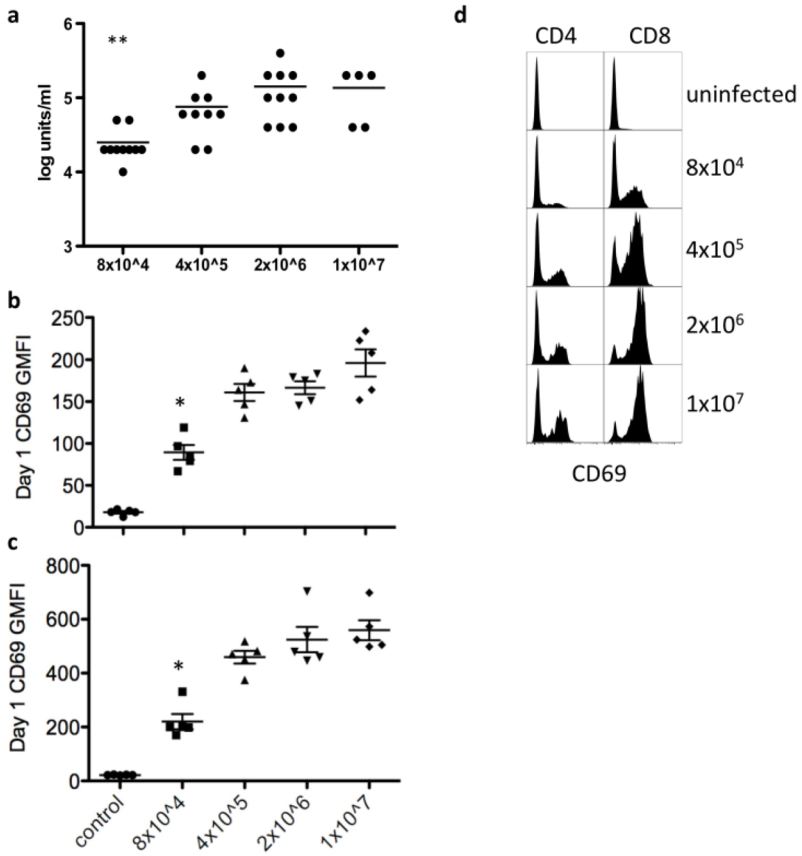

Figure 3. Differences type I IFN production and CD69 expression on CD4+ and CD8+ T cells

Mice were infected with 8×10^4 pfu, 4×10^5 pfu, 2×10^6 pfu or 1×10^7 pfu clone 13 i.v., or uninfected. **a.** Day 1 post infection type I IFN was measured using a bioassay. **b.** CD69 GMFI on CD4+ T cells, Day 1 post-infection. **c**. CD69 GMFI on CD8+ T cells, Day 1 post-infection. **d**. A representative histogram of CD69 expression on CD4+ and CD8+ T cells one day post LCMV cl-13 infection. Data are representative of 2–3 independent experiments. * $p<0.01$, ** $p<0.001$ by student T test.

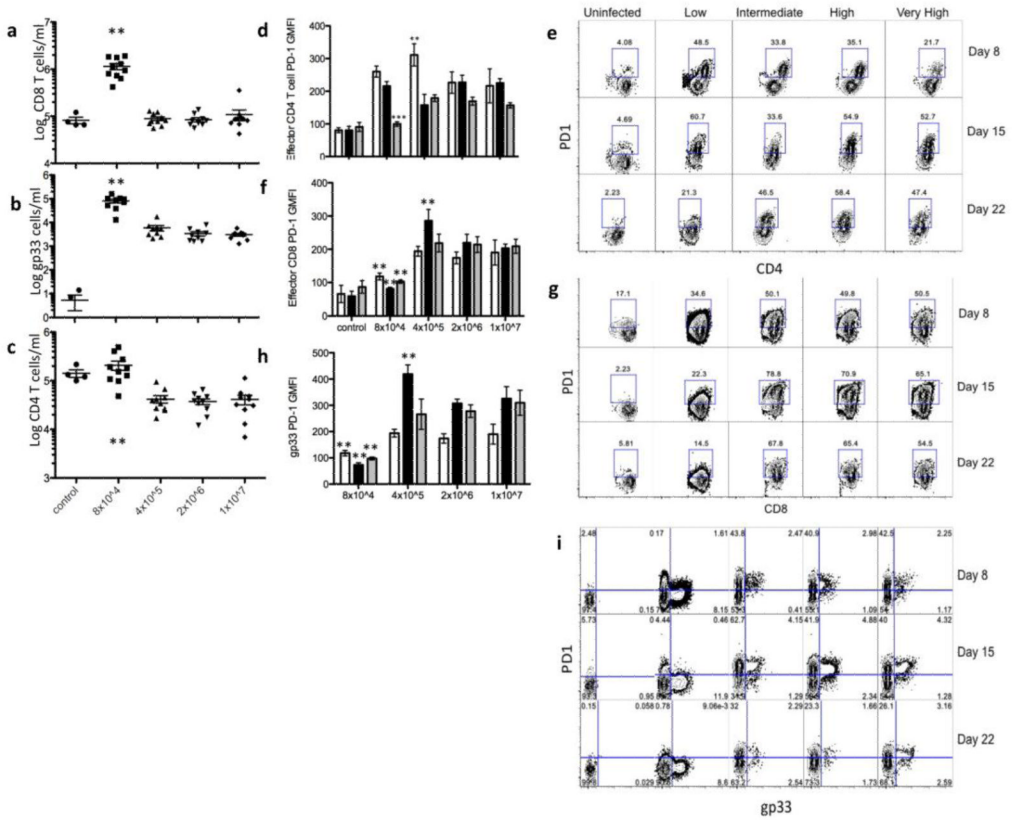

Figure 4. Differences in total peripheral T cells and PD-1 expression on CD4+ and CD8+ T cells

Mice were infected with 8×10^4 pfu, 4×10^5 pfu, 2×10^6 pfu or 1×10^7 pfu clone 13 i.v., or uninfected control. **a–c**. Day 8 post infection total cells/ml blood**. a.** Total CD8+ T cells. **b.** LCMV gp33 tetramer+ CD8+. **c.** Total CD4+ T cells. **d, f, h.** Day 8 (white bar), Day 15 (black bar) and Day 22 (gray bar) post infection PD-1 GMFI on **d**. CD44+ CD62L− CD4+ effector CD4+ T cells. **e.** Representative contour plots of effector CD4+ T cells. **f**. CD44+CD62L−CD8+ effector CD8+ T cells **g.** representative contour plots of effector CD8+ T cells and **h**. LCMV specific gp33 CD8+ T cells, plot gated on CD8+ effector T cells and **i.** representative contour plots of gp33 T cells gated on effector CD8+ T cells. Data are representative of 2–3 independent experiments. * $p<0.01$, ** $p<0.001$ ANOVA or student T test.

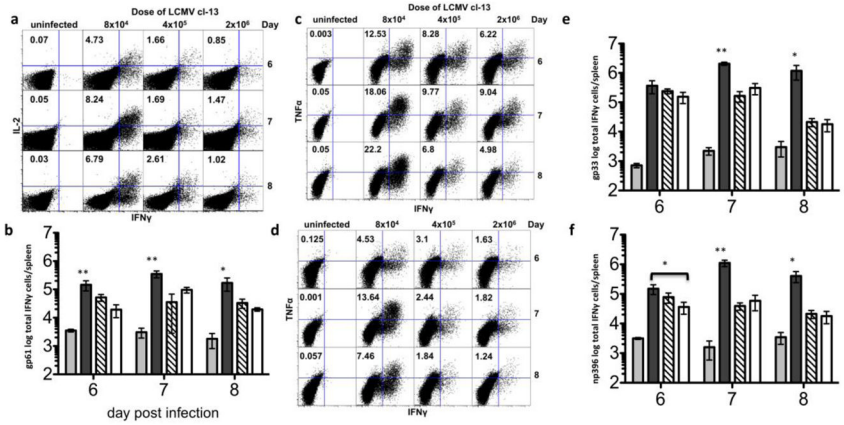

Figure 5. An early CD4+ T cell response is followed by a significant expansion of the CD8+ T compartment in mice infected with the low dose of cl-13

Mice were infected with a low (8×10^4 pfu), medium (4×10^5 pfu), high (2×10^6 pfu), or very high (1×10^7 pfu) dose of LCMV cl-13, or were uninfected (control). On days 6–8 post infection, some mice in each group were sacrificed and intracellular cytokine production by splenocytes was measured following in vitro LCMV peptide stimulation. **a**. gp61 stimulated splenocytes, gated on CD4+ T cells. Number indicates the percentage of CD4+ cells that were IFNγ positive. **b.** Total numbers of IFNγ producing cells were quantified in mice infected with uninfected control (grey bar), 8×10^4 pfu (black bar), 4×10^5 pfu (striped bar), or 2×10^6 pfu (white bar) following stimulation of CD4+ T cells with gp61. **c**. gp33 stimulated splenocytes, gated on CD8+ T cells. Number indicates the percentage of CD8+ cells that were IFNγ positive. **d.** np396 stimulated splenocytes, gated on CD8+ T cells. **E–f.** Total numbers of IFNγ producing cells were quantified in mice infected with uninfected control grey bar, 8×10^4 pfu (black bar), 4×10^5 pfu (striped bar), or 2×10^6 pfu (white bar) following stimulation; stimulation of CD8+ T cells with (**f**) gp33 or (**g**) np396. x axis indicates day post infection, error bars represent mean + SD. * $p<0.01$, ** $p<0.001$ student T. Results are representative of two independent experiments, n=4–5/group.

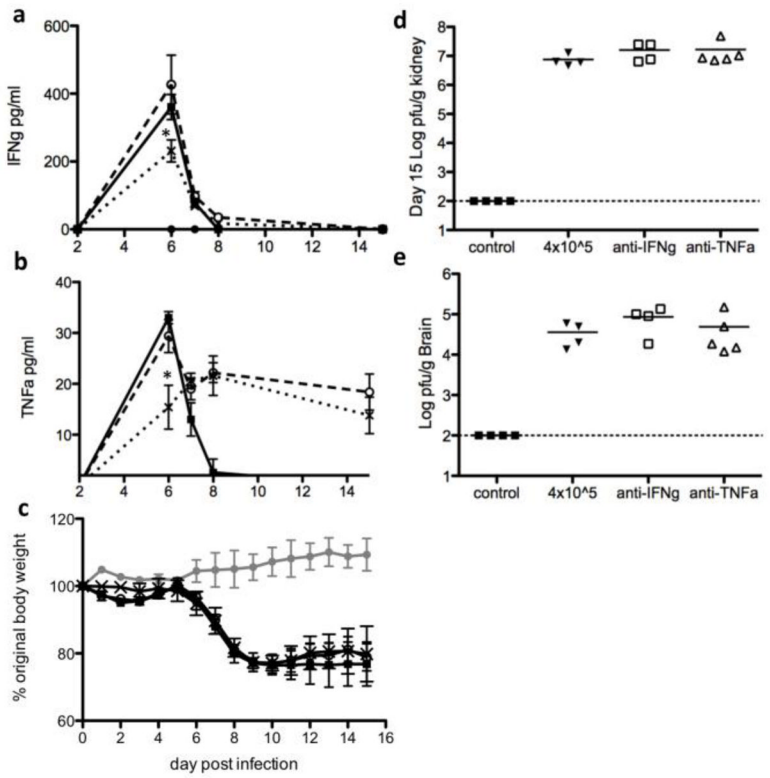

Figure 6. Levels of cytokines do not explain enhanced morbidity

a. IFNγ plasma levels as determined by a Luminex assay performed on samples taken from mice infected with 8×10^4 (■), 4×10^5 (○) or 2×10^6 pfu (×). (8×10^4 pfu p=0.0301 as compared to 2×10^6 pfu, student t –test) **b**. TNFα plasma levels, as determined by Luminex assay. Mice infected with $4x\times0^5$ pfu had a significant increase in TNFα (p=0.0498) on day 6 as compared to 2×10^6, (n=6/group). **c–e.** Mice were infected with 4×10^5 pfu of virus and treated on days 5 and 7 with either 200μg/treatment of anti-IFNγ or 100μg/treatment of anti-TNFα antibodies. **c**. Percentage body weight loss following treatment, grey is uninfected, untreated 4×10^5 pfu (■), anti-IFNγ (○) and anti-TNFα (×), error bars represent mean + SD. **d.** Kidney viral titers, day 15 post-infection. **e.** Brain viral titers, day 15 post-infection. Data are representative of two independent experiments, n=4–5/group.

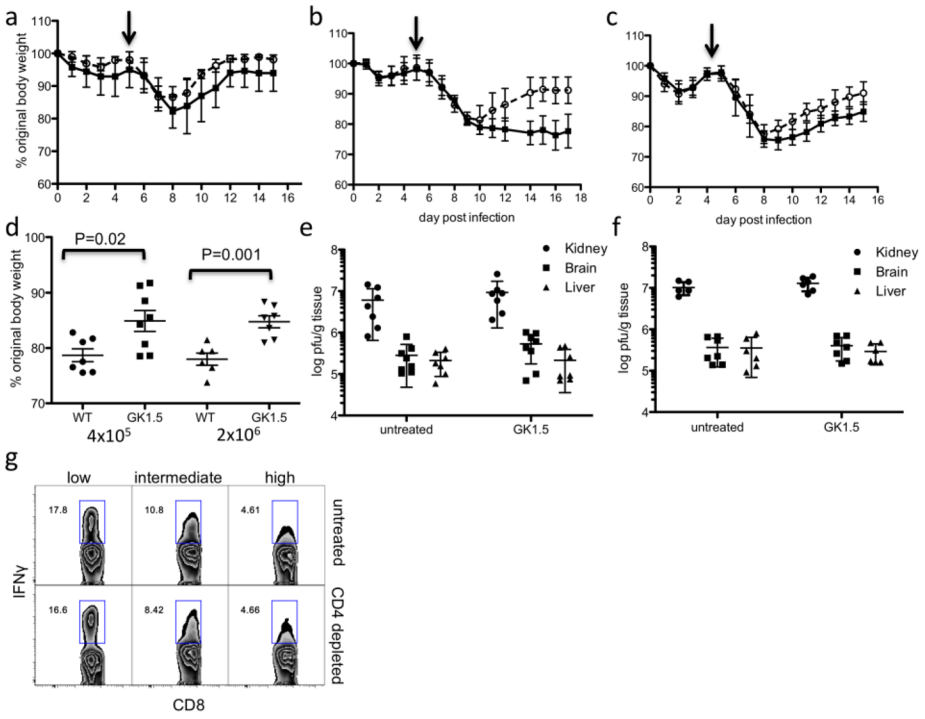

Figure 7. CD4+ T cells are required to maintain the wasting disease following a cl-13 infection

WT mice were infected with the low, intermediate or high LCMV clone 13. On day 5 post infection some mice were depleted of CD4+ T cells using the GK1.5 antibody (indicated by arrow). **a**–**c**. Percent loss of body weight of intact (solid line) or CD4-depleted (dashed line) animals infected with **a**. low, **b**. intermediate or **c**. high dose of cl-13. **d**. Day 11 post infection % body weight loss. All statistics were done using the student t-test. **e**–**f.** LCMV titers in tissues were measured 3 weeks after infection with **e.** Intermediate and **f**. high dose of LCMV cl-13. **d**. Representative plot of splenocytes that were stimulated with LCMV gp33 peptide and IFNγ production measured. Number indicates % of CD8+Thy1.2+ cells making IFNγ. All error bars indicate mean + SD. Data from two independent experiments displayed.

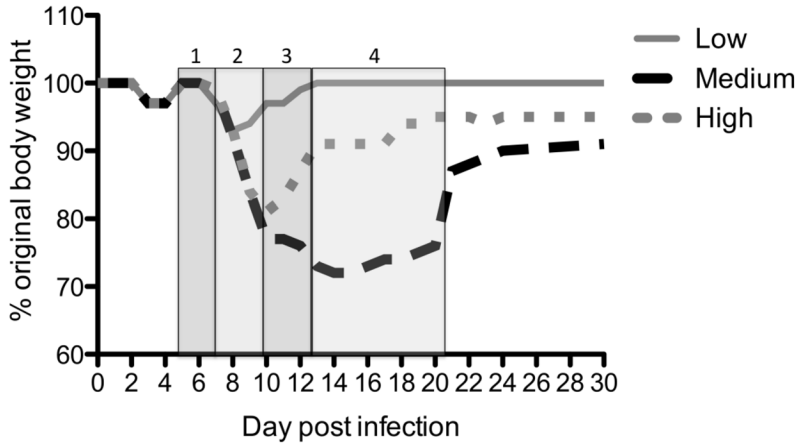

Figure 8. Proposed stages of morbidity following LCMV cl-13 infection

Mice infected with a low dose (8×10^4 pfu red), a medium dose (4×10^5 pfu blue) or a high dose (2×10^6 pfu green) of cl-13. % original body weight was monitored for 30 days post-infection. Stages: 1) initiation, 2) decline, 3) recovery, and 4) maintenance.